SCIENTIFIC REPORTS

OPEN

SUBJECT AREAS:
QUANTUM HALL
ELECTRONIC PROPERTIES AND DEVICES
APPLIED PHYSICS
SYNTHESIS OF GRAPHENE

Received
18 February 2013

Accepted
18 April 2013

Published
7 May 2013

Correspondence and requests for materials should be addressed to E.P. (emiliano.pallecchi@lpn.cnrs.fr)

Insulating to relativistic quantum Hall transition in disordered graphene

E. Pallecchi[1], M. Ridene[1,2], D. Kazazis[1], F. Lafont[3], F. Schopfer[3], W. Poirier[3], M. O. Goerbig[4], D. Mailly[1] & A. Ouerghi[1]

[1]CNRS - Laboratoire de Photonique et de Nanostructures, Route de Nozay, 91460 Marcoussis, France, [2]LPMC, Département de Physique, Faculté des Sciences de Tunis, Université Tunis-Manar, Campus Universitaire, 1060 Tunis, Tunisia, [3]Laboratoire National de Métrologie et d'Essais, 29 Avenue Roger Hennequin, 78197 Trappes, France, [4]Laboratoire de Physique des Solides, CNRS UMR 8502, Université Paris-Sud, 91405 Orsay, France.

Quasi-particle excitations in graphene exhibit a unique behavior concerning two key phenomena of mesoscopic physics: electron localization and the quantum Hall effect. A direct transition between these two states has been found in disordered two-dimensional electron gases at low magnetic field. It has been suggested that it is a quantum phase transition, but the nature of the transition is still debated. Despite the large number of works studying either the localization or the quantum Hall regime in graphene, such a transition has not been investigated for Dirac fermions. Here we discuss measurements on low-mobility graphene where the localized state at low magnetic fields and a quantum Hall state at higher fields are observed. We find that the system undergoes a direct transition from the insulating to the Hall conductor regime. Remarkably, the transverse magneto-conductance shows a temperature independent crossing point, pointing to the existence of a genuine quantum phase transition.

In two dimensional (2D) electron systems with an arbitrary weak elastic disorder, the scaling theory of localization predicts that at zero temperature all electron states are localized, resulting in an insulating system[1,2]. The transition from the high temperature regime characterized by a metallic behavior to the insulating one is still debated for 2DEGs[3] and is even more controversial for graphene, where the relativistic nature of the excitations should hinder localization, at least for certain types of disorder[4]. Nevertheless, experiments show that in the presence of intervalley scattering, electrons in graphene are subject to localization, with a crossover from strong localization[5] to weak localization[6] behavior when the localization length ξ increases far beyond the phase coherence length L_ϕ. The application of a perpendicular magnetic field can lead to the emergence of criticality in 2D disordered systems. At low field it increases the localization length by breaking the time reversal symmetry, it can therefore suppress localization. At high magnetic fields Landau levels are formed, with extended states near the band centers, which can account for electron transport in the quantum Hall (QH) regime. They also bring into play a new length scale, that is the magnetic length $l_B = \sqrt{\hbar/eB} \simeq 26/\sqrt{B[\mathrm{T}]}$ nm, here B is the magnetic field. Electron localization induced by disorder is also a key component of the QH effect, notably accounting for the finite width of the transverse magnetoresistance plateaus, and its role has been recently addressed in literature for graphene[7,8]. Here we discuss its relevance for the insulator-to-quantum Hall conductor (Ins-QH) transition at low field, where graphene proves itself as an ideal tool due to the robustness of Landau levels with respect to both disorder and temperature, arising from the large cyclotron gap $\Delta E_c = v_F\sqrt{2e\hbar B}$. The high field case has also been discussed in litterature[9]. The peculiarity of our samples is evident if we compare the Drude mobility of the graphene, where a fully developed QH effect was found, on the order of few hundred $\mathrm{cm^2V^{-1}s^{-1}}$, to that of the disordered 2DEGs where the Ins-QH transition has been generally observed, typically on the order of several to several tens of thousands $\mathrm{cm^2V^{-1}s^{-1}}$ [10–15].

Results

Graphene characterization. The two epitaxial graphene films that are used in our magneto-transport experiments were grown by thermal decomposition of SiC[16,17] and are mostly monolayer, with only a small fraction of bilayer, as evidenced by X-ray and angle-resolved photoemission spectroscopy (XPS/ARPES) measurements, shown in Fig. 1a (see also Methods and Supplementary information). One of the graphene films was exposed to molecular oxygen prior to the nanofabrication[18]. Our graphene films have a typical carrier concentration on the order of several 10^{12} $\mathrm{cm^{-2}}$ and feature a linear band dispersion, indicating that

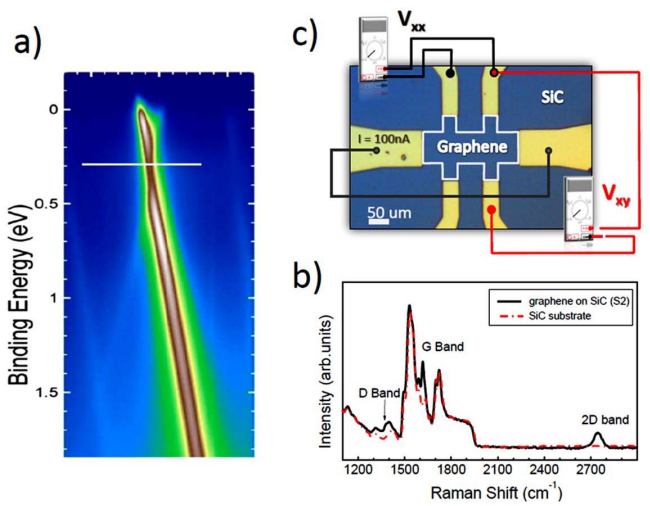

Figure 1 | Epitaxial graphene Hall bars. (a) ARPES spectra showing a linear dispersion. From the shift of the Dirac Energy $E_D = 0.3$ meV, measured with respect to the Fermi energy, we estimate a carrier concentration $n = E_D^2/(\pi\hbar^2 v_F^2) = 1.6 \times 10^{12}$ cm^{-2}. (b) Raman spectra of the graphene sample (black solid line) and of a SiC substrate (red dashed line). Contributions at the G and 2D band are observed, together with an important signal at the defect band D. (c) Sketch of the sample and principle of a Hall measurements, the longitudinal and Hall voltages V_{xx} and V_{xy} are measured for a fixed bias current I_b as a function of magnetic field. In the optical image of the finished device graphene is sketched in white, the size of the central region is 50 × 50 μm^2.

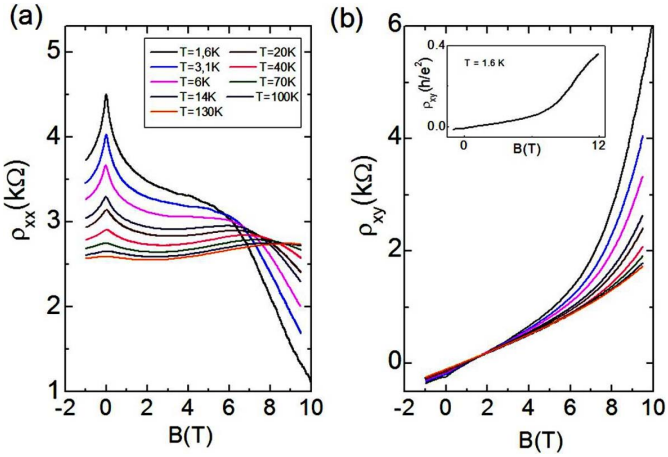

Figure 2 | Longitudinal and Hall magnetoresistance, diffusive sample S1. (a) Longitudinal magnetoresistivity measured during the first cooldown, for temperatures between 1.6 and 100 K. At low temperature the weak localization peaks develops. In this localized regime, resistance increases when decreasing the temperature. At higher fields the sign of the magnetoresistance depends on temperature: at low T the resistivity drops towards zero, indicating Hall effect, while at high temperature the magnetoresistivity has the opposite sign. (b) Hall resistivity, the kink around zero is due to the magnetic-field-symmetric term arising from a geometrical ρ_{xx} contribution. At higher fields ρ_{xy} becomes nonlinear anticipating the Hall plateau at $\upsilon = 2$. The nonlinearity increases strongly as the temperature decreases. In the inset a large B-sweep corresponding to the lowest temperature is shown.

despite disorder a crystalline graphene film is formed. These relatively low carrier concentrations (for epitaxial graphene) are required for observing the QH effect at accessible magnetic fields, on the order of several teslas. The presence of disorder is evidenced by contribution of the D band in the Raman spectra (Fig. 1b). The disorder in our samples is partially due to graphene edges and small fraction of bilayer. Since they both induce valley mixing, they favor localization at low temperatures. We used standard e-beam lithography, metal deposition, and dry etching to produce Hall bars with a large central region of 50 × 50 μm^2. A micrograph of one finished Hall bar is sketched in Fig. 1c, together with the principle of a Hall measurement.

Magneto-transport measurements: weakly disordered sample. In Fig. 2 we present the longitudinal and the transverse magnetoresistivity of the Hall bar S1, measured during the first cooldown of the sample. The data are recorded as a function of the applied perpendicular magnetic field for different temperatures, covering almost two orders of magnitude, from 1.6 K up to 100 K. The peak in the longitudinal resistivity ρ_{xx} at zero field is a manifestation of weak localization attesting the presence of significant valley mixing[5,19,20] and its large width of about 1 T is an indication of a short localization length. In such disordered samples, it turns out to be difficult to separate the Drude, weak localization, and the electron-electron contributions[21,22]. While an accurate fit of the weak localization has proven to be challenging, the estimated phase coherence length $L_\phi \approx 70$ nm at $T = 1.6$ K is close to typical values reported for graphene with short range disorder[5]. We also notice that the standard weak localization formula for graphene[19] may not be fully justified because the inter-valley short-range scattering seems to dominate over the intra-valley scattering. At high magnetic fields, ρ_{xx} decreases when the temperature is lowered because of the onset of Landau quantization. This is confirmed by the behavior of the Hall resistivity ρ_{xy}, which becomes highly nonlinear for large B, following the drop of ρ_{xx}, as expected before the appearance of a quantum Hall plateau. At low magnetic fields, the transverse resistivity ρ_{xy} varies about linearly. The kink in ρ_{xy} around zero field, which develops when the temperature is decreased, is due to a geometrical contribution of ρ_{xx} on ρ_{xy} (see Supplementary). It also leads to an apparent shift from zero of the ρ_{xy} curves crossing point. The sample gradually evolves from a more localized state towards the relativistic quantum Hall regime[23–25]. However, we do not find indications of a direct Ins-QH transition such as a temperature independent fixed point in the magnetoconductivity. This may result from the suppression of localization before the onset of the QH effect.

Direct Insulating to QH transition: strongly disordered sample. Consistent with this scenario, we find that the behavior is different for more disordered samples with lower carrier concentration. Here localization effects are more robust and Landau quantization develops at lower fields. In Fig. 3 we plot both the longitudinal and the Hall resistivity recorded at different temperatures, for two graphene Hall bars. The two data sets in Fig. 3 refer to sample S1 (Fig. 3 a–b), but when measured on a second cooldown, and to sample S2 (Fig. 3 a–b). The graphene film used for the latter was exposed to molecular oxygen prior to the Hall bar fabrication[18]. This treatment favors the observation of a direct Ins-QH transition. It decreases the carrier concentration of graphene and could enhance the number of short-range defects responsible for intervalley scattering[26]. Both samples exhibit the same qualitative behavior, the ρ_{xx} curves, which shows negative magnetoresistance as observed in disordered graphene in Ref. 27 are strongly affected by temperature and, remarkably, they all cross at a well-defined and T-independent magnetic field B_{c1}. Such a critical point suggests the existence of a zero-temperature quantum phase transition. Actually, at this field the sign of the temperature coefficient of the resistivity changes, identifying two regimes, a low-field insulating regime where the resistivity increases rapidly with decreasing temperature and a

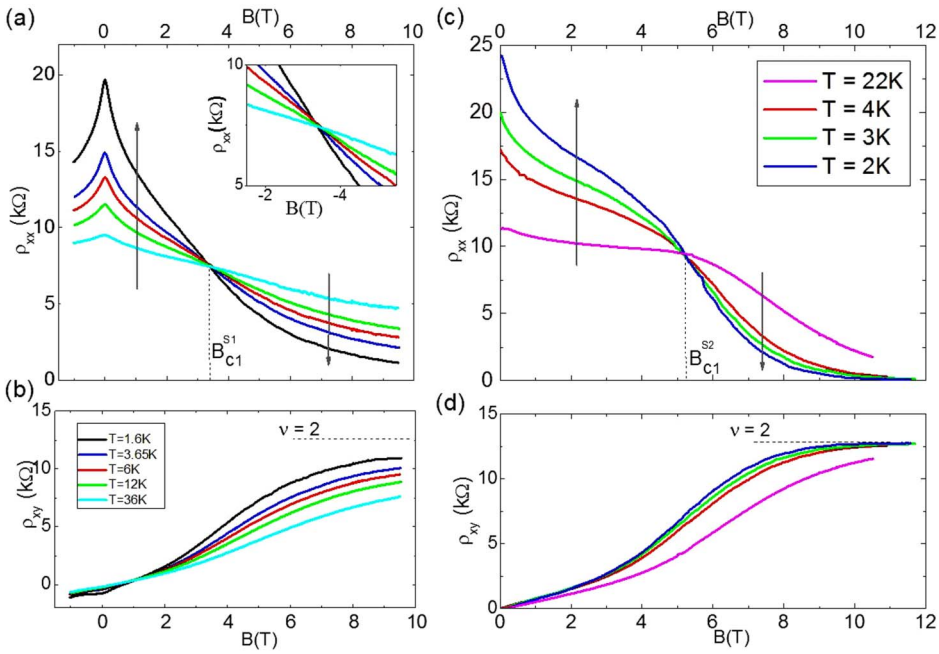

Figure 3 | Magnetoresistance, highly disordered samples. Longitudinal (a, c) and Hall (b, d) magnetoresistivity at different temperatures for sample S1-second cooldown and sample S2. The behavior is the same for both samples, with ρ_{xx} crossing at a well-defined, temperature-independent magnetic field $B_{c1}^{S1} = 3.3$ T and $B_{c1}^{S2} = 5.2$ T respectively. In the inset of (a) we show a zoom closer to the crossing point, data covers temperatures between 1.6 and 36 K. The sign of the temperature dependence of ρ_{xx} changes at B_{c1}, as symbolized by the vertical grey arrows.

quantum Hall regime at high fields, where the resistivity diminishes when T is decreased. The formation of a quantum Hall state at high fields is evidenced by the vanishing longitudinal resistivity and by the plateau on the Hall resistivity at a value $h/2e^2$.

We now focus on the data measured on device S2, since it displays a higher resistivity at zero field, suggesting a more localized state, and a better quantization of the Hall plateau. We start by estimating the carrier concentration $n = 1.2 \times 10^{12}$ cm^{-2} from the low-field Hall resistivity at 22 K, where localization and electron-electron interaction effects are less important. From the value of ρ_{xx}, still at 22 K, almost constant, equal to 10 kΩ, over 3 T-field range below B_{c1} where localization effects are further reduced, we also estimate the Drude resistivity $\rho_D \approx 8$ kΩ, by subtracting a small ≈2 kΩ-contribution ρ_{ee} from the electron-electron interaction[28]. The value of this contribution $\rho_{ee} = f\left(B, \rho_D, F_0^\sigma, c\right) \times \ln\left(k_B T \tau_{tr}/\hbar\right)$ can be calculated with the number of multiplet channels participating in the interaction reduced to $c = 3$ by the strong intervalley scattering, the Fermi-liquid constant F_0^σ, which is the interaction parameter, equal to -0.1, as usually reported in literature for graphene[21,29,30], and $\tau_{tr} = l_{tr}/v_F$ the transport time deduced from ρ_D. The consistency of the values calculated for ρ_{ee} and ρ_D was checked a posteriori. The transport scattering length calculated from the Drude resistivity, which does not include localization effects, is short, as we find $l_{tr} = h/(2e^2 \rho_D \sqrt{\pi n}) = 15$ nm. The Drude mobility is $\mu = 1/\rho_D n e =$ 860 cm^2/Vs.

The graphene zero-field resistivity $\rho_{xx}^{B=0}$ of the order of h/e^2 at low T, much larger than its Drude value of 8 kΩ, indicates that quantum interferences are a dominant feature in electron transport, leading to a strong localization at low T. This is confirmed by the small value of the localization length $\xi \sim 50$ nm estimated using the relation $\xi = l_{tr} \exp\left(h/e^2 \rho_{xx}^{B=0}\right)$[5,31]. Interestingly, X_{si} appears very close to the transport length l_{tr}. All these features indicate a stronger localization of electrons at low magnetic field than in the first cooldown of sample S1, with the insulating behavior of localized states in 2D graphene being manifested by the high value of the resistivity at zero magnetic field and its strong temperature dependence. The appearance of the plateau at Landau level filling factor near $\nu = nh/eB = 2$ in the high field Hall magnetoresistance is also important. It confirms that despite the low mobility, the Landau levels are sufficiently quantized to still manifest the chiral Dirac fermions character in the magnetotransport measurements. While not exactly identical to the ratio of the cyclotron energy separating the Landau band centers to the disorder broadening of the bands themselves, the classical quantity $\omega_c \tau_{tr}$, with ω_c the cyclotron pulsation, is commonly used to estimate the magnetic field where Landau level quantization becomes sensitive considering that at this point $\omega_c \tau_{tr} = 1$. To some extent, this criterion should also apply to determine the critical magnetic filed of the Ins-QH transition. However, for samples S1 (second cooldown) and S2, the transition occurs at $B_{c1}^{S1} = 3.3$ T and $B_{c1}^{S2} = 5.2$ T respectively, for $\omega_c \tau_{tr} = 0.2$ and 0.34 respectively, with $\omega_c = eBv_F/\hbar\sqrt{n\pi}$. Even if the transition is frequently observed for $\omega_c \tau_{tr} < 1$ in disordered 2DEGS[11,13–15,32], the very low $\omega_c \tau_{tr}$ value found in those graphene samples at the transition is remarkable. This could be attributed to the anticipated onset of the robust graphene quantum Hall effect at $\omega_c \tau_{tr} \ll 1$ which requires an in-depth study, notably because it is also an asset for certain applications, such as the quantum Hall metrology[33]. More generally, the occurrence of the Ins-QH transition at magnetic field lower than expected also questions the relevance of the criterion $\omega_c \tau_{tr} = 1$ to determine the position of this transition. It is worth noting that, near the magnetic field B_{c1}, the magnetic length l_B, for example equal to 11.5 nm in S2, is close to our estimation of the localization and the transport scattering length. This confirms l_B, X_{si}, l_{tr} are a meaningful T-independent criterion to estimate the position of the Ins-QH transition.

Discussion

The crossing point in the longitudinal magnetoresistance has already been interpreted as the signature of a QPT in 2DEGs. Such interpretation has been questioned by Huckestein[34], who proposed a scenario with a smooth crossover due to the suppression of weak localization. Electron-electron interaction and weak localization corrections to the longitudinal conductivity in cleaner samples can also

originate a fixed crossing point in the longitudinal resistivity due to the conductivity/resistivity tensor conversion. However, in our experiments the strong nonlinear character of ρ_{xy} which anticipates the fully developed $\nu = 2$ plateau at high fields proves that Landau quantization is already important at fields as low as 3 T, much smaller than the crossing point field $B_{C1}^{S2} = 5.2$ T, suggesting that the QHE is a key ingredient of the transition observed. It has been suggested that a stronger indication of the QPT could be obtained by the analysis the magnetoconductivity data[35], which are linked to the resistivity by the relations $\sigma_{xx} = \rho_{xx} \Big/ \left(\rho_{xx}^2 + \rho_{xy}^2\right)$ and $\sigma_{xy} = -\rho_{xy} \Big/ \left(\rho_{xx}^2 + \rho_{xy}^2\right)$. The main advantage here is that the transverse conductivity σ_{xy} is not affected by electron-electron interaction corrections. In addition, in the scaling theory of the QHE, these are some values of σ_{xy} which behave as fixed points under renormalization[36]. Magnetoconductivity curves for sample S2 are plotted in Figure 4. The shift in the longitudinal conductivity (Fig. 4a) reveals the presence of electron-electron interactions. The presence of a T-independent crossing point in the transverse magnetoconductivity (Fig. 4b) which is observed at a field $B_{C2} = 4.5$ T close to B_{C1}^{S2}, strongly hints to a quantum phase transition. In addition, such a fixed point on $\sigma_{xy}(B)$ has been observed on sample S1 (second cooldown) which is claimed to undergo a direct Ins-QH transition, and not in the first cooldown when a gradual crossover occurs.

It is therefore tempting to analyze our data near the critical point using the scaling theory of the quantum Hall effect[37], which is known to capture the physics of the delocalization-localization transitions in both 2DEGs and graphene. The divergence of the localization length is described by a power law $\xi \propto (E - E_c)^{-\gamma}$, where E_c is the energy of the delocalized state at the center of the Landau level. The exponent γ is not easily accessible, but is linked to the parameter $\kappa = p/2\gamma$, where p, usually taken to be 2 for graphene[2], describes the temperature dependence of the phase coherence length $L_\phi \propto T^{-p/2}$. The critical exponent for the Ins-QH transition κ can be extracted from magnetoconductivity data which are expected to scale with temperature according to $\propto T^{-\kappa}$ at the critical magnetic field[11,14]. In the case of sample S2, κ was simply extracted from the linear fit of the $\ln(d\sigma_{xy}/dB)$ versus ln(T) plot at B_{C2}, as shown in the inset of Fig. 4 b. The data follow the expected linear relation, and κ, equal to the slope of the fit was found to be 0.26 ± 0.03. This experimental value of κ is in good agreement with what is reported for more conventional 2DEGs, in the case of spin-degenerate Landau levels and dominant short-range disorder, for the Ins-QH transition[11,14], as well as for QH plateau to QH plateau transitions[2,36,38]. This seems to suggest that the low-field insulator to QH transitions, QH to QH transitions and QH to high-field insulator transitions belong to the same QPT universality class.

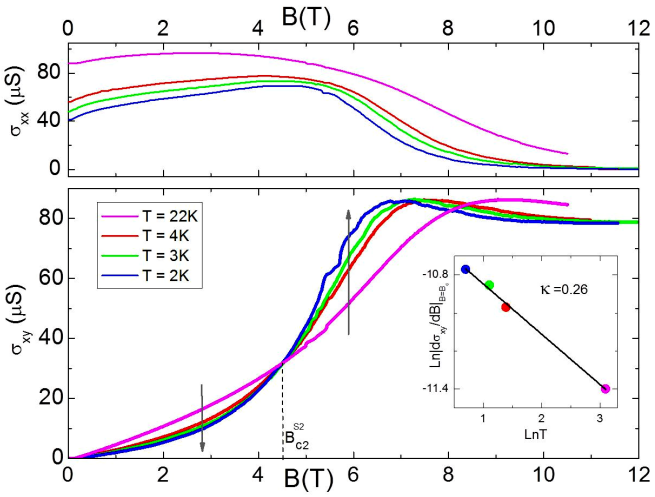

Figure 4 | Extraction of the critical exponent kappa. Longitudinal (top) Hall and (bottom) Hall magnetoconductivity, for different temperature, sample S2. The Hall term also shows a well defined crossing point at $B_{c2}^{S2} = 4.5$ T. The slopes of $\sigma_{xy}(B)$ scales with temperature at B_{c2} according to $\propto T^{-\kappa}$. The critical exponent equal to $0.26 \pm xx$ is extracted from the fit of these slopes as shown in the inset.

Thus, we have shown that for low-mobility graphene with resistivity on the order of h/e^2 a direct transition between a localized and the quantum Hall regime is induced by the magnetic field. Analysis of the magnetoconductivty hints to a genuine quantum phase transition, rather than a simple crossover. The transition can be described by a scaling law with a critical exponent of 0.26. Thanks to its large cyclotron gap, robust to strong disorder graphene is the material of choice for the study of the Ins-QH transition. Such a study could unveil new aspects of the metal-insulator transition in two-dimensional systems due to the relativistic nature of graphene carriers.

Methods

The graphene was grown by thermal decomposition of an undoped 4H-SiC(0001). The substrate was first etched in a hydrogen flux at 1500°C at 200 mbar for 15 min in order to remove any damage caused by surface polishing and to form a step-ordered structure on the surface. After the etching, the substrate was transferred into an ultrahigh vacuum (UHV) chamber with a base pressure of 10^{-9} mbar. The surface of the substrate was annealed at 600°C during 60 min. The substrates were heated under a Si flux (1 ML/min) at 800°C to remove the native oxide in UHV (P = 2 10^9 mbar). Graphene was synthesized by exposing the substrate an argon flux at 1350°C under semi-UHV (P = 210^5 mbar) during 15 minutes. This induces a growth of a $\left(\sqrt{3} \times 6\sqrt{3}\right)$ R30°, and $\left(6\sqrt{3} \times 6\sqrt{3}\right)$ R30° reconstructions as an intermediate step towards few layer growth of graphene due to Si depletion. The temperature of the substrate was calibrated with an infrared pyrometer in the high temperature range and with a thermocouple in the low temperature range. XPS and ARPES experiments were performed in ultra high vacuum conditions at TEMPO beamline at the SOLEIL Synchrotron facility (Saint-Aubin, France). The Hall bars were structured using standard e-beam lithography and PMMA was used as resist. The etching was performed by a 15 seconds exposure to oxygen plasma in our reactive-ion etching setup. For the electrodes we deposited a palladium-gold bilayer 20/80 nm, followed by lift-off in thrichloroethylene.

1. Abrahams, E., Anderson, P., Licciardello, D. C. & Ramakrishnan, T. Scaling Theory of Localization: Absence of Quantum Diffusion in Two Dimensions. *Physical Review Letters* **42**, 673–676 (1979).
2. Evers, F. & Mirlin, A. Anderson transitions. *Reviews of Modern Physics* **80**, 1355–1417 (2008).
3. Smet, J. H. Metalinsulator transition: A plane mystery. *Nature Physics* **3**, 370–372 (2007).
4. Ponomarenko, L. A. *et al.* Tunable metal-insulator transition in double-layer graphene heterostructures. *Nature Physics* **7**, 958–961 (2011).
5. Moser, J. *et al.* Magnetotransport in disordered graphene exposed to ozone: From weak to strong localization. *Physical Review B* **81**, 205445 (2010).
6. Morpurgo, A. & Guinea, F. Intervalley Scattering, Long-Range Disorder, and Effective Time-Reversal Symmetry Breaking in Graphene. *Physical Review Letters* **97**, 196804 (2006).
7. Martin, J. *et al.* The nature of localization in graphene under quantum Hall conditions. *Nature Physics* **5**, 669–674 (2009).
8. Jung, S. *et al.* Evolution of microscopic localization in graphene in a magnetic field from scattering resonances to quantum dots. *Nature Physics* **7**, 245–251 (2011).
9. Chekelesky, J. C. *et al.* Zero-Energy state in graphene in a High Magnetic Field. *Physical Reviez Letters* **100**, 206801 (2008).
10. Jiang, H., Johnson, C., Wang, K. & Hannahs, S. Observation of magnetic-field-induced delocalization: Transition from Anderson insulator to quantum Hall conductor. *Physical Review Letters* **71**, 1439–1442 (1993).
11. Wang, T., Clark, K., Spencer, G., Mack, A. & Kirk, W. Magnetic-field-induced metal-insulator transition in two dimensions. *Physical Review Letters* **72**, 709–712 (1994).
12. Gusev, G. *et al.* Absence of delocalised states in a 2D electron gas in a magnetic field below $\omega_c\tau = 1$. *Solid State Communications* **100**, 269 (1996).
13. Song, S., Shahar, D., Tsui, D., Xie, Y. & Monroe, D. New Universality at the Magnetic Field Driven Insulator to Integer Quantum Hall Effect Transitions. *Physical Review Letters* **78**, 2200–2203 (1997).
14. Huang, C. *et al.* Insulator-quantum Hall conductor transitions at low magnetic field. *Physical Review B* **65**, 3–6 (2001).
15. Liang, C.-T. *et al.* On the direct insulator-quantum Hall transition in two-dimensional electron systems in the vicinity of nanoscaled scatterers. *Nanoscale research letters* **6**, 131 (2011).
16. Berger, C. *et al.* Electronic confinement and coherence in patterned epitaxial graphene. *Science* **312**, 1191–6 (2006).

17. Ouerghi, A. *et al*. Epitaxial graphene on 3C-SiC(111) pseudosubstrate: Structural and electronic properties. *Physical Review B* **82**, 125445 (2010).
18. Mathieu, C. *et al*. Effect of oxygen adsorption on the local properties of epitaxial graphene on SiC (0001). *Physical Review B* **86**, 1–5 (2012).
19. McCann, E. *et al*. Weak-Localization Magnetoresistance and Valley Symmetry in Graphene. *Physical Review Letters* **97**, 14–17 (2006).
20. Aleiner, I. L. & Efetov, K. B. Effect of Disorder on Transport in Graphene. *Physical Review Letters* **97**, 236801 (2006).
21. Lara-Avila, S. *et al*. Disordered Fermi Liquid in Epitaxial Graphene from Quantum Transport Measurements. *Physical Review Letters* **107**, 166602 (2011).
22. Eroms, J. Comment on Evidence for Spin-Flip Scattering and Local Moments in Dilute Fluorinated Graphene. *Physical Review Letters* **109**, 179701 (2012).
23. Zhang, Y., Tan, Y.-W., Stormer, H. L. & Kim, P. Experimental observation of the quantum Hall effect and Berry's phase in graphene. *Nature* **438**, 201–4 (2005).
24. Novoselov, K. S. *et al*. Two-dimensional gas of massless Dirac fermions in graphene. *Nature* **438**, 197–200 (2005).
25. Goerbig, M. Electronic properties of graphene in a strong magnetic field. *Reviews of Modern Physics* **83**, 1193–1243 (2011).
26. Pallecchi, E. *et al*. Observation of the quantum Hall effect in epitaxial graphene on SiC(0001) with oxygen adsorption. *Applied Physics Letters* **100**, 253109 (2012).
27. Hong, X. *et al*. Colossal negative magnetoresistance in dilute fluorinated graphene. *Physical Reviez B* **83**, 085410 (2011).
28. Kozikov, A. A., Savchenko, A. K., Narozhny, B. N. & Shytov, A. V. Electron-electron interactions in the conductivity of graphene. *Physical Review B* **82**, 075424 (2010).
29. Jobst, J., Waldmann, D., Gornyi, I. V., Mirlin, A. D. & Weber, H. B. Electron-Electron Interaction in the Magnetoresistance of Graphene. *Physical Review Letters* **108**, 106601 (2012).
30. Jouault, B. *et al*. Interplay between interferences and electron-electron interactions in epitaxial graphene. *Physical Review B* **83**, 195417 (2011).
31. Kivelson, S., Lee, D.-H. & Zhang, S.-C. Global phase diagram in the quantum Hall effect. *Physical Review B* **46**, 2223–2238 (1992).
32. Shahar, D., Tsui, D. & Cunningham, J. Observation of the $\upsilon = 1$ quantum Hall effect in a strongly localized two-dimensional system. *Physical Review B* **52**, R14372–R14375 (1995).
33. Schopfer, F. & Poirier, W. Graphene-based quantum Hall effect metrology. *MRS Bulletin* **37**, 1255–1264 (2012).
34. Huckestein, B. Quantum Hall effect at low magnetic fields. *Physical Review Letters* **84**, 3141–3144 (2000).
35. Hughes, R. J. F. *et al*. Magnetic-field-induced insulator-quantum Hall-insulator transition in a disordered two-dimensional electron gas. *Journal of Physics: Condensed Matter* **6**, 4763–4770 (1994).
36. Huckestein, B. Scaling theory of the integer quantum Hall effect. *Reviews of Modern Physics* **67**, 357–396 (1995).
37. Pruisken, A. Universal singularities in the integral quantum Hall effect. *Physical Review Letters* **61**, 1297–1300 (1988).
38. Koch, S., Haug, R., Klitzing, K. & Ploog, K. Size-dependent analysis of the metal-insulator transition in the integral quantum Hall effect. *Physical Review Letters* **67**, 883–886 (1991).

Acknowledgments

We acknowledge B. Etienne for fruitful discussions. We thank F. Sirotti, M.G. Silly for the XPS and ARPES experiments. We are grateful to U. Gennser for stimulating discussions and for proofreading our manuscript. D. Kazazis acknowledge LNE financial support within the action incentive contract LNE/10-3-002. This work was supported by the the French Contract No. ANR-2010-BLAN-0304-01-MIGRAQUEL, the French-Tunisian CMCU project 10/G1306, and the RTRA Triangle de la Physique.

Author contributions

E.P. and A.O. planned the experiments. A.O. fabricated the graphene layer and characterized it by XPS and ARPES. D.K. and E.P. produced the Hall bars, E.P., D.K., M.R. conducted the measurements, F.L., F.S., W.P. carried out complementary experiments. E.P., M.R., M.O.G., F.S., W.P. and A.O. analyzed the data, D.M. supported the experiment. E.P. wrote the paper with all authors contributing to the final version. A.O. supervised the project.

Additional information

Supplementary information accompanies this paper at http://www.nature.com/scientificreports

Competing financial interests: The authors declare no competing financial interests.

License: This work is licensed under a Creative Commons Attribution-NonCommercial-NoDerivs 3.0 Unported License. To view a copy of this license, visit http://creativecommons.org/licenses/by-nc-nd/3.0/

How to cite this article: Pallecchi, E. *et al*. Insulating to relativistic quantum Hall transition in disordered graphene. *Sci. Rep.* **3**, 1791; DOI:10.1038/srep01791 (2013).